frontiers | Frontiers in Energy Research

TYPE Original Research
PUBLISHED 09 January 2023
DOI 10.3389/fenrg.2022.1025045

OPEN ACCESS

EDITED BY
Muhammad Amjad,
University of Engineering and Technology, Pakistan

REVIEWED BY
Fahad Noor,
University of Engineering and Technology, Pakistan
Muhammad Aftab Akram,
Pak-Austria Fachhochschule Institute of Applied Sciences and Technology, Pakistan
Amjad Hussain,
University of Engineering and Technology, Pakistan
Binghong Chen,
University of Shanghai for Science and Technology, China

*CORRESPONDENCE
Jianfeng Huang,
huangjf@sust.edu.cn

SPECIALTY SECTION
This article was submitted to Solar Energy,
a section of the journal
Frontiers in Energy Research

RECEIVED 22 August 2022
ACCEPTED 23 September 2022
PUBLISHED 09 January 2023

CITATION
Syed N, Feng Y, Fahad R, Sahito IA and Huang J (2023), Carbon nanomaterials staked with nonwoven (EG/PAN/CQDs) composite as a counter electrode for enhanced photons and photocatalytic efficiency.
Front. Energy Res. 10:1025045.
doi: 10.3389/fenrg.2022.1025045

Carbon nanomaterials staked with nonwoven (EG/PAN/CQDs) composite as a counter electrode for enhanced photons and photocatalytic efficiency

Noureen Syed[1,2,3], Yongqiang Feng[1], Raja Fahad[2], Iftikhar Ali Sahito[3] and Jianfeng Huang[1]*

[1]School of Materials Science and Engineering, Shaanxi University of Science and Technology, Xi'an, China, [2]Department of Textile Engineering, Mehran University of Engineering and Technology, Jamshoro, Pakistan, [3]Center of Excellence in Nanotechnology and Materials, Mehran University of Engineering and Technology, Jamshoro, Pakistan

Prior studies on heavy metal heterojunction with carbon nanomaterials for dye-sensitized solar cells (D-SSCs) found that they were not only toxic but also had poor stability and led to a difficult synthesis. In this work, nanomaterials with flexible nonwoven sheets were employed to improve cell efficiency and were easily synthesized with high stability, durability, washability, and flexibility. By incorporating carbon quantum dots (CQDs) into the anode and counter electrodes, it is possible to boost photon efficiency by scattering the sunlight and turning a huge amount into current density. Here in this research, Textile carbon–based flexible dye-sensitized solar cells (TC-DSSC) with N-doped CQDs may significantly increase solar cell efficiency. Carbon-based nanoparticles stacked with textile apparel (nonwoven bamboo) sheets enabled the desired flexible end applications to be achieved. The prepared material significantly increased solar cell efficiency to 11.26% compared to 8.04% of the one without CQDs. Carbon-based nanomaterials are stacked with textile apparel (nonwoven bamboo) sheets to make them lightweight, highly flexible, wearable, and user-friendly. Furthermore, compared to pure expanded graphite on the nonwoven substrate, a single electrode incorporating CQDs offered low impedance and high current/voltage. On the other hand, when tested for photocatalytic activity using spectrophotometry, the proposed counter electrode made of expanded graphite, PAN, and CQDs loaded on nonwoven material completely degraded the methylene blue dye in a very short period of time. The N-CQDs may prove to be very stable with outstanding washing endurance anchored with expanded graphite layered on a nonwoven medium with an optimum thickness.

KEYWORDS

photovoltaic properties, CQDs (carbon quantum dots), DSSC (dye-sensitized solar cell), photocatalytic activity, expanded graphite, carbon nanomaterial

Introduction

For photovoltaic devices, many approaches have been put forth to date; however, a promising strategy to meet third-generation demand (especially for solar cells) that enables low-cost and improved long-term stability in DSSC with ease of manufacturing provides to expand research area. Polymer-based or apparel-based photon devices have recently received a lot of interest in producing flexible devices. Fabrics covered with carbon nanomaterials have demonstrated excellent flexibility and deformability for shaping into almost any shape and integrating with any portable electronic equipment as a sustainable power source, in contrast to traditional solar cells with a planar structure (Brown et al., 2014; Fu et al., 2018; Sadasivuni et al., 2019). The electrical conductivity of improved graphite staked with carbon quantum dots (CQDs) is a potential attraction to conventional solar cells of carbonaceous materials with flexible bases induced charge transfer process; it efficiently decomposes methylene blue dye.

The exceptionally low toxicity, chemical inertness, and excellent power conversion efficiency of CQDs make them a special class. Nanostructures, such as nanosheets, nanorods, mesoporous films, and nano-sized dots, are being incorporated into textile apparel to enhance the surface area, act as a barrier against redox reactions, and work as conductive junctions. Due to their simplicity to manufacture, low-cost, theoretically high power conversion efficiency (Sahito et al., 2015a), and minimum environmental impact, textile carbon–based dye-sensitized solar cells (DSSCs) have attracted a lot of attention (Saravanan et al., 2017; Heo et al., 2018; Lv et al., 2022) (Ahmed et al., 2020; Mousa et al., 2022). The key to increasing the efficiency of this research is tailoring the CQDs utilized as electrodes (Li et al., 2019; Sharif et al., 2022). One of the best solutions to replace costly platinum (Pt) electrodes in a dye-sensitized solar cell is as follows: counter electrode (CE) may be covered with CQDs prepared by expanded graphite by combining nonwoven sheets, producing a typical solar cell that comprises economic benefits over other solar cells. Therefore, to find cost-effective materials, carbon-based nanomaterials, polymers, and compounds are more effective. To create highly effective flexible wearable solar cells with nanomaterials that are user-friendly (Sahito et al., 2015b), skin-friendly, light-weight, and powerful solar cell output devices, it is crucial to customize the selection of electrode designs and materials (Guo et al., 2017; Singh and Shougaijam, 2022). It has been proven that carbon materials are an excellent solution to resolve the issues raised above. However, pure expanded graphite is very inexpensive and conductive with less electro-catalytic nature; therefore, fulfilling synchronized character by incorporation of CQDs has been achieved (Riaz et al., 2019). Additionally, in this work, nanostructured electronics were effectively incorporated into textile constructions to expand the application and replace costly FTO- and Pt-based electrodes. In addition, CQDs, with their unique luminous property, may be employed to enhance photovoltaic qualities (Sahito et al., 2016). The CQDs produce electrons that are widely used in circuits, catalysis, photovoltaics, storage devices, and other applications when exposed to light irradiation (Guo et al., 2017; Zhang et al., 2018; Li et al., 2019; Khan et al., 2020; Ramanujam et al., 2020; Lv et al., 2022; Sharif et al., 2022; Singh and Shougaijam, 2022). The photo-excitation performance and, consequently, electron concentration of the final CQDs are considerably increased by doping CQDs with N elements. For wearable DSSC to be highly effective, the clarity and flexibility of the front electrode must be improved (He et al., 2020). There has not been a lot of published research on improving the front electrode's transparency in stacked-type solar cells. Only a small percentage of photons were able to stimulate and adjust the semiconductor's electron-hole separation in the majority of the suggested system, which used a back illumination strategy. Here, we describe a stacked and expanded graphite carbon structure–based dye-sensitized solar panel (TC-DSSC). A highly transparent and conductive carbon front electrode (CFE) was made *via* CQDs functionalization, and solar system–produced TiO_2 that had been hydrothermally coated with CQDs that contained natural dye was examined for photovoltaic activity (Peerakiatkhajohn et al., 2016; Kandi et al., 2017; Kong et al., 2018).

Additionally, cathode composite has been suggested for photocatalytic activity and demonstrated 100% methylene blue dye degradation under UV light for 10 ppm solution in 25 min only. Testing on nonwoven clothing textiles has been performed to establish their physical enhancement, which includes flexibility, durability, and stability (Fu et al., 2018; Tao et al., 2019). The recommended TC-DSSC showed 4% higher efficiency compared to TG-DSSC, and CQDs containing solar cell efficiency demonstrated increased photovoltaic performance with a high Jsc of 19.60 mA cm^{-2}. Investigations on the impact of charge transport and all electrochemical characteristics on solar cells were extensive. The produced C-DSSC is incredibly adaptable and can be incorporated or sewn into clothing for wearable batteries, power gadgets, or self-powered medical devices. The proposed study provides an example of a straightforward flexible solar cell for future needs.

Experimental

Materials

Transparent fluorinated tin oxide glass (FTO) was used for the C-DSSC assembly, and a nonwoven bamboo sheet was utilized. Sodium nitrate ($NaNO_3$, close to 100%), concentrated sulfuric acid (H_2SO_4, 98%), hydrogen peroxide (H_2O_2, 35%), polyacrylonitrile (PAN), concentrated hydrochloric acid (36.5%),

and methylene blue dye were purchased from Sigma Aldrich. Graphite powder was bought from Bay Carbon, United States. For the electrolyte spacer, iodide electrolyte and 40 μm surlyn sheet were used for assembling the electrode.

Fabrication of photo anode electrode

To get more photon-containing electrodes, the CQDs-based front electrode (CFE) was meticulously constructed to obtain better efficiency and sheet conductivity requirements. Various CFE sheets with varying carbon quantum dots content weight percentages were prepared for this purpose. First, five FTO glass electrodes of 2 × 2 cm^2 size were washed with ethanol and water and mixed in a 1:1 ratio. The CF FTO was ultrasonically washed for 2 h and then dried for another 2 h. The washed CF FTO were clamped by tape for applying TiO^2 paste. Paste preparation was carried out by thoroughly mixing 10 mL of ethanol and TiO^2 powder till a smooth paste was realized. Furthermore, TiO^2 containing FTO electrodes was prepared, and to get scalpel printing thickness up to 6–8 μm thick, a coat was applied, and vacuum heat was applied at different temperatures i.e., low to high (70–450°C). The baked coated glass was cooled down to around 70°C. Afterward, CQDs containing dye solution were prepared. For dyeing, natural strawberries were meshed in an extractor, and strawberry juice was taken out, vacuum filtered, and kept at a temperature of 100°C. CQDs dye-containing solution was prepared by 1:1 stock solution and immersed into TiO_2 coated FTO glass for 24 h under the dark.

Fabrication of textile-CQDs dye-sensitized solar cell and precursors synthesis

Carbon-based textile solar cells are highly demanded due to their flexibility and higher electrical conductivity with long stability. For achieving all these characteristics and improved electrochemical efficiency, different composites were examined in this work. Nonwoven, as a base material compared with woven cloth material, is highly approachable because of having high thermal stability and excellent absorbency and providing a smooth structure. To get high conductivity and photo electron properties, initially, five 2 × 2 cm^2 of fabric were cut into pieces and washed with acetone and water, respectively. They were then dried and tape-casted using 40-, 60-, and 80-mm tape. The expanded graphite paste was evenly spread on the substrate using the doctor blade method, and the practice was continued till a homogenous coating was achieved. The graphite-coated fabric was then clamped with another tape, and PAN (polyacrylonitrile) nanofiber dip CQDs were coated on a graphite nonwoven sheet. The absorbed PAN by CQDs enables the graphite paste to be more stable, improves its deposition, and enhances its efficiency. However, for strong bonding, air drying was realized at 150°C for 2 hours in a dry oven.

Graphite oxide (GO) is a byproduct of graphite oxidation processes like Hummer's method, as given in our previous work (Sahito et al., 2016). The graphite crystal structure was synthesized to include oxygen-containing groups (epoxide and hydroxyl) by oxidizing it. Because these oxygen groups interact with water, the GO becomes hydrophilic. Water is introduced between the GO sheets due to their hydrophilicity, causing them to disperse easily. For synthesis, graphite (5 g) was put into a flask with 2.5 ml of sodium nitrate and 115 ml of sulfuric acid (high immaculateness grade). The suspension was mixed under a magnetic stirrer for 30 min at 0 °C (the suspension tone was dark). Then, the mixture was left for 3 days at room temperature. For making the mixture highly oxidized, this suspension was treated with water (the shade of the suspension changed to more dispersed, and the suspension turned out to be more porous). 10 ml of water was added to the flask, and the entire stock was left for 30 min at room temperature. Afterward, 21 ml of hydrogen peroxide (reagent grade) was added. The mixture become more expanded, and the shade of the acquired suspension changed to light grey. After the solution was conditioned for 24 h at room temperature, it was filtered over and again and washed with refined water. The filtered cake was thermalized using a microwave oven at a high temperature until it turned out highly conductive. This thermal heating of waves with high temperatures made the cake highly expanded.

Using the dip-and-dry coating process, a stock solution was created before creating the cathode electrode. 3 mg of GO particles were diluted in the stock solution and sonicated for 30 min to make the solution. The nonwoven cut sheet was dipped into the solution for 20 min, dried at 100°C for 15 min, and then repeated dip coating to achieve high loading. Additionally, GO/nonwoven requires stability, an improved electrical channel, and an active site with strong bonds without redox capability and CQDs with PAN coating were used as a second layer. PAN nanofibers were made using the electrospinning process followed by previously reported work (Yang et al., 2010). In brief, PAN was dissolved in DMF solvent with 12% polymer and was used to produce nanofibers through electrospinning. This solution was agitated for 24 h to ensure homogenous mixing. A 5 ml syringe with a tiny tip that measured 0.5 mm across the inward distance was used to inject the electrospinning fluid. A collector and a high voltage of 15 kV were employed in conjunction with the needle's drops to produce an electric field that was exceedingly concentrated. Aluminum foil 0.5 mm thick was used to cover a metal plate that served as the collector and was connected by terminals. The collector was configured with a 15 cm working distance. A syringe pump was used to regulate the polymer arrangement's flow rate. The 1 ml/h flow rate was the most effective (Li et al., 2016; Jiao et al., 2019; Mahala et al., 2020; Lv et al., 2021), and for CQDs, the synthesis process was followed

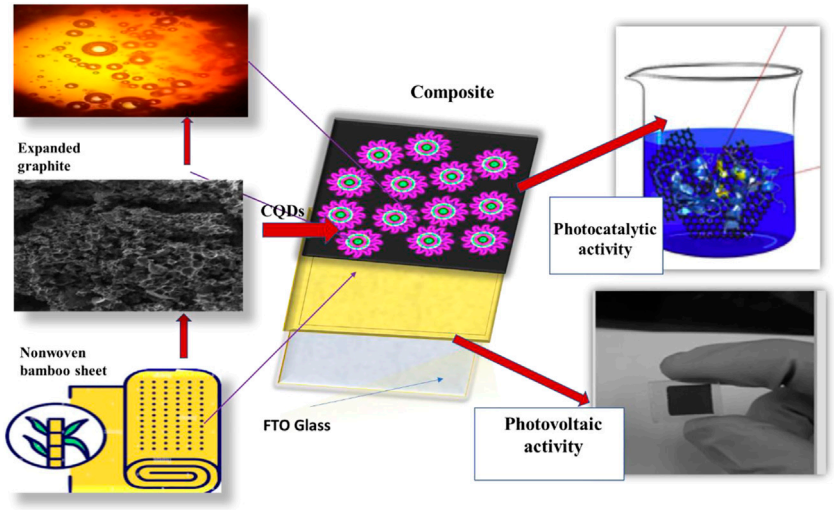

FIGURE 1
Schematic illustration of composite to experimental work.

by a previously reported work. The hydrothermal approach has been used to synthesize N-CQDs (Cao and Yu, 2016; Lu et al., 2018; Ren et al., 2019). In brief, 3 g citric acid and 3 g urea (0.11 wt%) was placed in a measuring beaker. Then, 30 ml of deionized water was added, the suspension was placed in a magnetic stirrer for 5 min at room temperature, and the homogeneous solution was moved into a 100 ml hardened steel reactor with a Teflon liner for the quick aqueous response at 140–240°C for 2–10 h, respectively. After cooling to ambient temperature, the final suspension was filtered through a 0.22 μm filter paper to remove big particles. Then, it was transferred to a 20 ml dialysis machine (1 kDa sub-atomic weight cutoff) and dialyzed in 1.5 L purified water several times for 48 h, yielding a pale-yellow N-CQD solution.

The second layer of CQDs loaded PAN nanofibers was applied by making stock solution, and the dip solution coating method was used again to coat this nanofiber layer on the graphite oxide layer. PAN nanofibers were repeatedly dip coated, followed by drying at 70°C to get high absorbency of CQDs on PAN nanofibers. For combining the nonwoven, loaded GO was first clamped, and PAN/CQDs were pasted on it accurately with the same size of 2 × 2 cm^2.

To avoid short circuits in textile CQDs dye-sensitized solar cells (TC-DSSC), the fibrous structure of the cathode should exceed interfacial contact, or it may cause short circuits and lead to low photovoltaic activity. To lower this risk, a gel type of electrolyte was prepared as a polymer electrolyte (Sahito et al., 2017). For the preparation of the polymeric electrolyte, PVA was dissolved in water with a 1:1 ratio. The synthesized electrolyte was added and continuously stirred until a homogenous polymer-containing electrolyte was obtained following the full dissolution of PVA and gel formation. Using a syringe, the electrolyte was injected into the closed assembly of (TC-DSSC). All procedures are explained by schematic illustration, as shown in Figure 1.

Characterizations

The microstructure and surface morphology of the precursors and PAN/CQDs/GO nonwoven were recorded by transmission electron microscopy (TEM) and scanning electron microscopy (SEM, JEOL model JSM 6010 LA) instrument operated at an accelerating voltage of 10 kV. EDX was attached to FESE, with EDX to analyze the presence of nanoparticles on the surface of PAN nanofibers. XRD was performed using a Rigaku RINT-2000 diffractometer with a source of filtered Cu Ka radiation. XRD pattern of graphene oxide (GO) was also examined. All precursors were analyzed by different characterizations. For CQDs, the particle size and size distribution were examined by using the Zeta sizer (Malvern Zeta Sizer Nano ZS series, United Kingdom) by dispersing nanoclusters at a temperature of 25 °C in aqueous media. The Origin Pro 8.5 and ImageJ software were used for data analysis, curve fitting, and fiber diameter distribution. UV and FTIR (FTIR, Shimadzu, 8900-FT-IR spectrometer Tokyo Japan) were also taken for further confirmation. Dye photodegradation was examined using a Hitachi UV–vis spectrophotometer (UV-2700, Shimadzu, Japan) at a wavelength from 200–700 UV-visible spectra of the methylene blue (MB). The proposed sample's electrical resistance was examined using a resistive test instrument of a typical four-

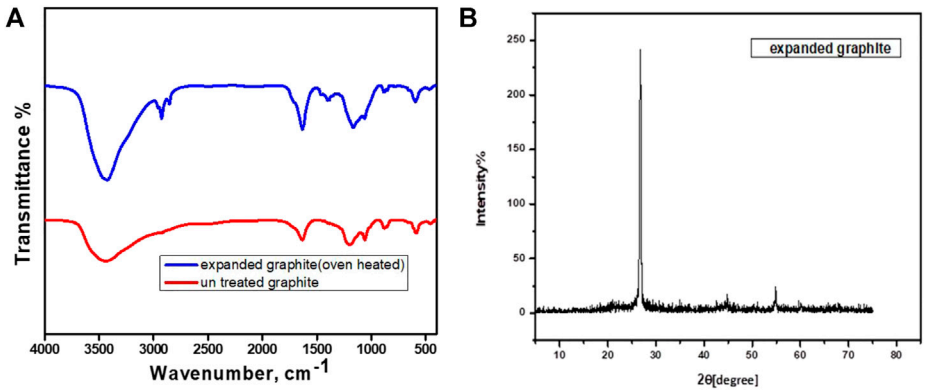

FIGURE 2
(A) FTIR of pristine graphite and expanded graphite. **(B)** XRD graph of GO (graphite oxide).

probe head system, and the thickness of layers was examined with an FTO glass using a micrometer. Using the electrochemical impedance spectroscopy (EIS) method, the charge transfer resistance (RCT) at the DSSC cathodes was examined by using the electrochemical impedance spectroscopy (EIS) technique. The efficiency of a TC-DSSC prepared by expanded graphite stacked with CQDs/PAN nanomaterials was measured using a device (Mac science CO) equipped with a solar simulator with a 160 W xenon arc lamp as a solar simulator.

Result and discussion

Schematic illustration Characterization of expanded graphite oxide

The FITR spectra of expanded graphite were obtained using Fourier transform infrared spectroscopy (FTIR), as illustrated in Figure 2A. Peaks that signify the presence of O-H stretching C-O carboxyl may be detected on 3,436 cm^{-1}, 2,921 cm^{-1}, 1,285 cm^{-1}, 164 cm^{-1}, 1,394 cm^{-1}, and 1,164 cm^{-1}. Treated graphite with OH groups improved mild to strong C=C stretching and peak definition and height. The existence of C=C is indicated by a minor absorption at 2,116 cm^{-1} in pure graphite in comparison. The O-H group is present, as indicated by the maximum wavelength of 3,438 cm^{-1} in expanded graphite. Additionally, a solid wave number of 870 cm^{-1} produced by C-H bending vibrations and the presence of weak C=C at a wavelength of 2,116 cm^{-1} were found, while pure graphite was discovered to be less absorbent and to have fewer hydroxyl groups.

On the other side, Figure 2B shows the XRD pattern for synthesized expanded GO. Here, the very strong and very sharp diffraction peak around 26.5° is assigned to the (002) diffraction peak of the plane reflection. It is confirmed that the (002) diffraction peak of the expanded graphite corresponds to the characteristic peak. This peak shows the highly active site availability in graphite structure because of thermal decomposition of intercalation compounds of graphite made highly oxidized.

Characterization of CQDs

The nano size particles and size distribution of the CQDs samples were examined by using the Zeta sizer. The CQDs with a typical size of 340 nm were uniformly distributed and monodispersed, as shown in Figures 3A and B. CQDs were discovered to be formed by oxidative cleavage into the homogeneous size of particles that have been widely dispersed. The size distribution of CQDs was in the range of 400–500 nm, with the content of CQDs reaching up to 35%. On the other hand, for structure understanding, of synthesized CQDs, as prepared by citric acid and urea, ultimately form strong carbon-based materials. Because of a strong chain of sp^2 bond present in urea, which is utilized for doping of N-doped CQDs, and a further citric acid is also a basic form of C=C/C-C, which is present in CQDs main structure, and all these bonds after thermal heating reach to the surface of the nucleus of CQDs. To confirm these functional groups, the presence of (-OH), carboxyl (-COOH), and carbonyl (-C=O) in the primary structure of CQDs was established by FTIR analysis. The FTIR spectrum validates the oxygen functionalities of different types by distinguishing different peaks. 3,450 cm^{-1} (O-H stretching vibrations), 2,902 cm^{-1}, 2,852 cm^{-1} (C-H stretching vibrations), 1,625 cm^{-1} (C-Stretching), and 3,219 cm^{-1} (peak) (N-H stretching). These findings suggest that CQDs arise by the breakdown of epoxy groups and the underlying C–C bonds. Based on these findings, we can conclude that formed CQDs are N-doped and C=C/C-C

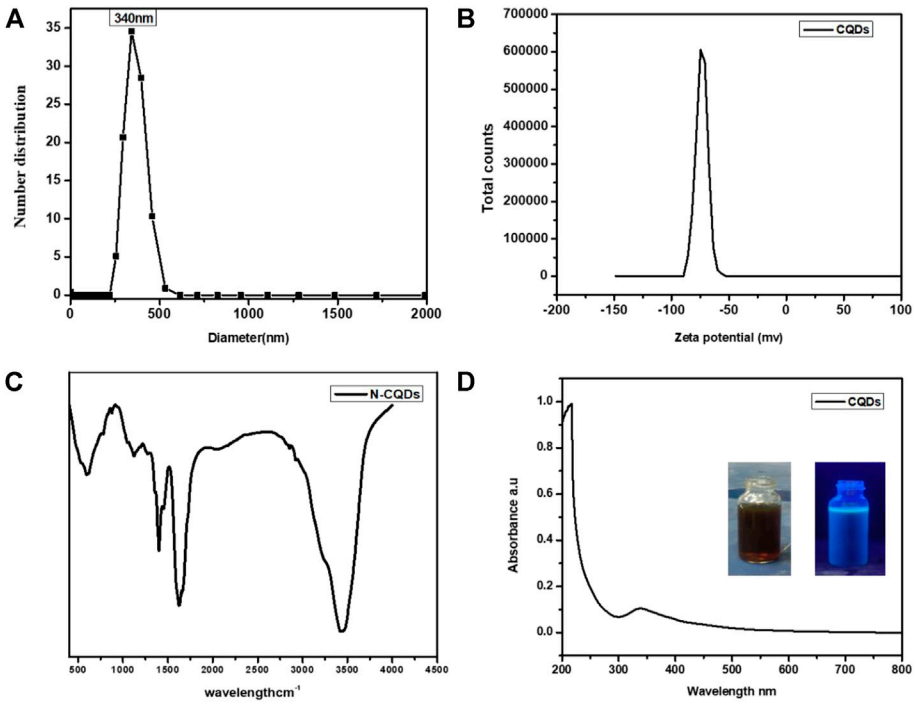

FIGURE 3
(A) Size analyzer of CQDs 3. **(B)** Zeta Potential of CQDs 3. **(C)** U-V light of CQDs3. **(D)** FTIR of CQDs.

with hydrogen bonding and that all these bonds fluctuate with hydrothermal temperature and time. Because of the carbonyl and hydroxyl groups, it is readily soluble. Furthermore, when UV-vis absorbance was used to analyze optical properties, it was discovered that the maximum absorption was seen at 340 nm (Figure 3C), which was the aromatic system's absorption and had previously been reported to have a high PL on this wavelength, and the water-soluble CQD had fine optical properties that were observed under UV-light. They emit a light brown tint throughout the day and a blue color when exposed to UV light, making them nontoxic and environmentally acceptable and considering them as alternatives for semiconductor quantum dots to be applied in the photocatalytic application. The hydrophilic nature made this a more suitable candidate for absorbency base photodegradation of MB. Moreover, N-doped CQDs, for their photoexcitation performance, enhanced the efficiency of solar cells by increasing dye electron density accelerating photovoltaic properties and the microstructure of CQDs on solar cell and on CE. This symmetrical study reveals the influence of CQDs on the efficiency of the cell.

Characterization of composite

Figure 4 summarizes several characterizations, including SEM, EDX, and TEM images of expanded graphite, PAN, and PAN/GO/CQDs composite nanofibers. SEM in Figure 4A verified the highly expanded and porous structure of graphite. After chemical treatment and thermal heating, it collapsed the graphite layer and deformed the structure randomly, resulting in high porosity and smoothness in the structure. Figures 4B and C show SEM of PAN nanofibers (b) without coating and (c) with coating, demonstrating fine, smooth, and uniform composite nanofibers with an average diameter in nm and clear difference with pristine PAN and treated PAN with CQDs. The morphology of TC-DSSC composite nonwoven complete electrode by the cross-sectional view, as displayed in Figure 4D, also demonstrates that the fine layering of graphite containing PAN with CQDs is smoothly pasted on the nonwoven structure. Figure 4E demonstrates the cross-sectional and top view PAN nanofibers loaded with CQDs taken after making a complete electrode of samples; the obtained product changed into a counter electrode shape.

Furthermore, the presence of CQDs on PAN nanofibers was investigated using a TEM image. Figure 4F confirms that nano-sized particles dispersed smoothly on the surface. In addition, the microstructure and morphology of the nanofibers were analyzed using an EDX analyzer. It was discovered that the presence of highly expanded graphite oxide and CQDs increased conductivity and photovoltaic and made the nanofiber surface highly porous, which helped to increase the active surface area

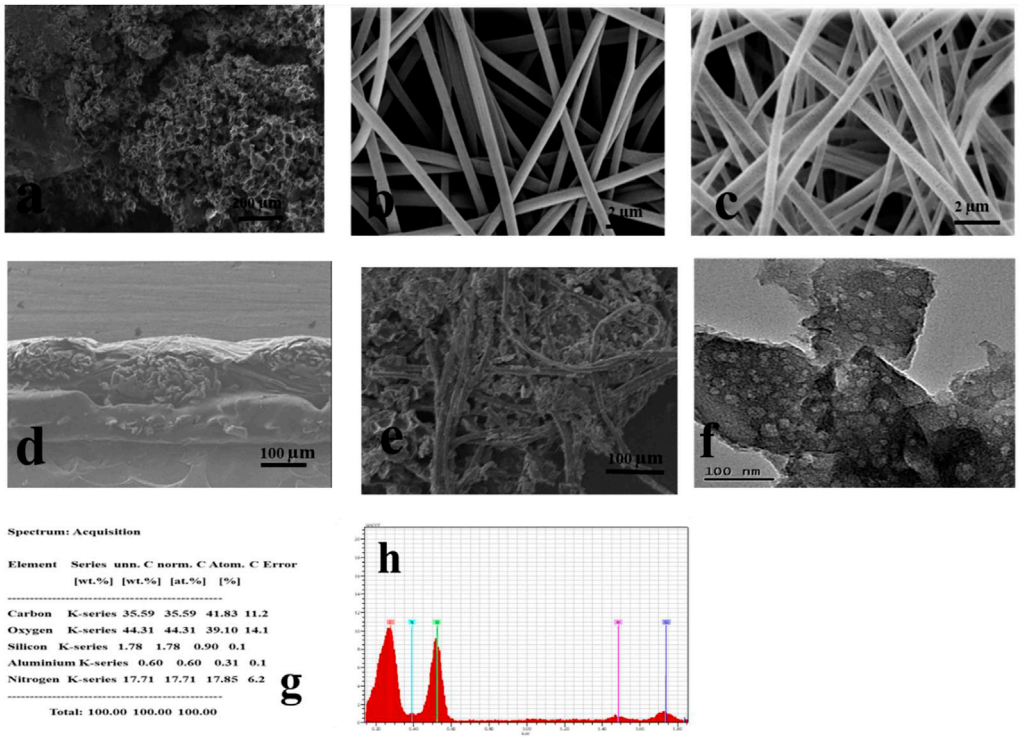

FIGURE 4
Morphology of composite **(A).** SEM of expanded graphite **(B and C).** SEM of PAN nanofibers **(D and E).** Cross-sectional and front view of composite **(F).** TEM image of CQDs with PAN **(G and H).** X-ray (EDX) of composite.

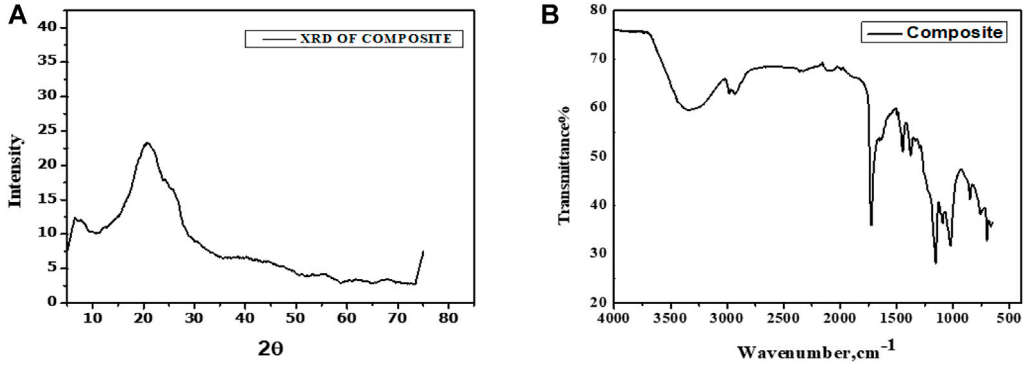

FIGURE 5
(A) XRD of composite. **(B)** FTIR of composite.

and improve the efficiency of DSSC. The layers of GO and CQDs are seen to be smooth. This cross-linked network forms a fibrous web with a wide surface area for dye absorption. To confirm the distinct elements present in the composite nonwoven sheet, an energy dispersive X-ray (EDX) examination of the composite was performed. The acquired EDX spectra are shown in Figures 4G and H, revealing the basic elements carbon (C), nitrogen (N), and oxygen (O) atoms.

In addition, X-ray diffraction was used to study the crystalline structure of the PAN/GO-CQDs nonwoven film, as shown in Figure 5A. The crystalline character of the composite was confirmed by the strong peaks at 2Θ values of 22.55°.

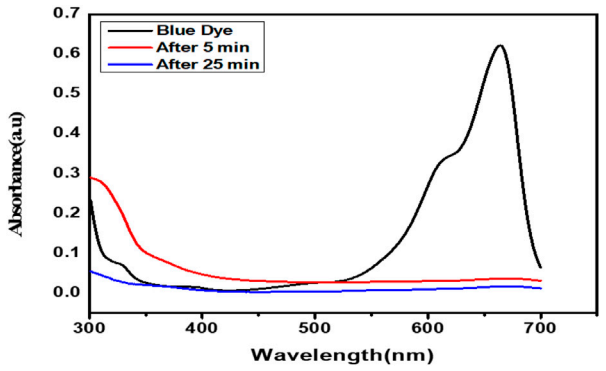

FIGURE 6
UV light of photodegradation of methylene blue.

Furthermore, one notable peak at 2Θ of 30° indicates the presence of a C-C bond, indicating that the film is substantially rich in carbon (Othman et al., 2016). On the other hand, Figure 5B shows the FTIR spectra of CQDs/PAN nanofiber coated expanded graphite/nonwoven composite. The band at 1,050 cm^{-1}, which is attributable to the symmetric stretching of CQDs and GO on PAN, can be observed in a composite. While the peak at 3,252 cm^{-1} is caused by the aromatic rings' C-H stretching vibration in GO, the peak at 1,551 cm^{-1} is caused by the -C, N, and O groups in a composite. Peaks at 2,921 cm^{-1} and 2,850 cm^{-1} correspond to strong stretching of N-H, while peaks at 1968 cm^{-1} and 2000 cm^{-1}, respectively, represent medium stretching C=C=C. Due to C-N stretching in aromatic amines, which is an indication of crosslinking, the peak at 1,149 cm^{-1} confirms the existence of aromatic amine groups in expanded graphite/PAN nanofibers. The wide band vibrates when stretched. It is possible to attribute the peak at 1,551 cm^{-1}. Because of the existence of CQDs, the peak at 1,551 cm^{-1} can be attributed to N-O asymmetric stretching.

Fabrication of expanded graphite nonwoven photocatalyst

A spectroscopy absorption approach was used to analyze the photocatalytic degradation of MB dye. A 250 ml cylindrical quartz vessel was filled with aqueous solutions of the catalyst support counter flexible electrode FTO free and the MB dyes (0.10 g/L, 100 ml). Additionally, the solution was added and stirred continuously for various time ratios to mix and mobilize the dye on the surface of the nanofibers with different time ratios. To accomplish the adsorption–desorption equilibrium of MB on the composite surface, the suspension was stirred mildly without visible light illumination. A 300 W Xenon light with a frequency from 400 to 700 nm served as a light source (Alley et al., 2012; Khalid et al., 2017; Qu et al., 2018). The separation from the light source to the fluid surface was set to 15 cm. The change in dye concentration was studied and analyzed using dye absorbance of color in UV spectra photometer after 5 min and 25 min, as shown in Figure 6. To evaluate the photocatalytic degradation of methylene blue under visible light and UV light irradiation in a photocatalytic reactor, CQDs/PAN/GO nanofibers were used. An orbital shaker, a beaker with dye solution, and a light source positioned as shown make up the photoreactor. The UV lamp was turned on to start the photocatalytic reaction, and any other lights were shielded throughout the process. A UV-visible spectrophotometer was used to record changes in the absorbance band of the MB spectrum at the specified time intervals and analyze the photo-reacted solution.

Washable textile-embedded flexible carbon-based solar cell

The light weight, flexibility, shatter resistance, and stability of textile-based solar cells with high specific power voltage are their key characteristics (Fu et al., 2018; Heo et al., 2018; Lv et al., 2022; Singh and Shougaijam, 2022). Here, in this work, we produced a combination of inexpensive and essentially usable carbon nanomaterials combined with flexible textile apparel for comfortable use on textiles. Researchers are looking for more flexible materials to replace the hard glass in the part of the light-blocking layer in order to get electrodes with greater transparency and higher efficiency (Li et al., 2019). It is anticipated that flexible energy materials would fundamentally alter how we use energy, transforming our way of life. A significant component is the fabrication of the cell process. Among several techniques, dye-sensitized solar cells stacked with fabric coated with CQDs were thought to be a hot study issue. With the addition of N and S, the photoexcitation and photovoltaic performance of DSCC are improved (Yang et al., 2014).

Without the need for battery maintenance or recharging, solar cells might make textile-based wearable devices energy-independent; however, their washing resistance, which is a requirement for consumer adoption of e-textiles, has rarely been explored. The purpose of this research is to present a thorough investigation of the launder ability of solar cells incorporated into fabrics. Because of their soft, flexible, light, air-permeable, elastic, and stretchable qualities, which are adaptable to human body forms and movements, textiles offer a natural substrate for wearable technology. Textiles are resilient to a variety of environmental factors and weather conditions, as well as rigorous handling, folding, bending, and processing. Additionally, clothing and textiles are subjected to prolonged, densely packed storage, spilling onto the ground, exposure to sunshine, chemicals, and the most demanding conditions. Textiles and clothing also resist prolonged, densely packed

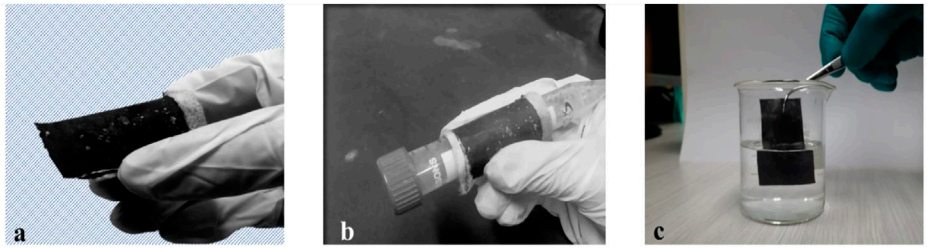

FIGURE 7
(A) Complete flexible counter electrode **(B).** Flexibility checked by wrapping on cylinder **(C).** Washing durability testing.

storage, falling to the ground, exposure to sunshine, chemicals, and the most difficult laundry washing.

E-textile do not follow standard testing of washing, hence, ISO 6330:2012 (SFS-EN ISO 6330:2012, 2012) must be followed (Rotzler et al., 2021), but these methods are difficult to follow; according to standards on our samples, the testing technique was followed by soaking electrodes in detergent water for 72 h at room temperature. As a result, it revealed good washing durability and found no material bleeding in the water. Martindale abrasion test and pilling test were carried out as suggested by different authors (Fu et al., 2018; Tao et al., 2019; Rotzler et al., 2021). These tests may be useful from the perspective of the textile industry to forecast the robustness against mechanical stress and water tightness of individual electrical components or sensor materials. While for flexibility checking wrapped electrode on a cylindrical tube, both methods were chosen to prove washing durability and flexibility of electrode as shown in Figure 7.

Photovoltaic testing

In this work, a brand-new and simple method for creating wearable dye-sensitized solar cells has been proposed. The CCE cathode of the metal-free solar panel was separated by membrane spacers that had been hydrated with polymer electrolytes. To assess the compatibility of manufactured electrodes for C-DSSC, a photo anode and cathode's ability was estimated before the complete C-DSSC was made. Different comparison studies of solar cells were created. The solar cell fabrications include (1) full TC-DSSC (with CQDs), (2) TG-DSSC (without the addition of CQDs) graphite coated on nonwoven, and (3) symmetrical cells comparison with CQDs and without CQDs. Nyquist plots were plotted using the Z-view software (Fu et al., 2018; Tao et al., 2019; Ahmed et al., 2020; Rotzler et al., 2021; Saberi Motlagh et al., 2022), and electrochemical testing was determined by calculating using an equivalent circuit. The improved photoelectric conversion efficiencies in the counter electrode front, that are predominantly attributed to the increased electron concentration from photo exciting N-CQDs and, consequently, photovoltaic performances of light-inducing CEs, are confirmed by results that show TC-DSSC impedance at CCE/CQDs. The maximum efficiency for TC-DSSC is 11.84% for CQD solar cells and 8.84% for TG-DSSC without CQDs, respectively. However, DSSC without addition of CQDs layer on cathode layer, it was coated with graphite sheet staked with nonwoven sheet, reduction of CQDs from both electrode was also analyzed and showed higher impedance, while with addition of CQDs on both electrodes in a shape of complete cell was examined, its analyzed by comparing lower impedance of due to higher electron excitation as shown in Figures 8A–C which confirms high current voltage with low impedance for CQDs containing solar cell, because the incident light passed through CQDs generate high electrons and increase absorbency of dye molecules and regulate this process fast to excite electron towards conduction band and CQDs with its photo luminous sufficiently energize to excite and hindered the electron recombine with holes during the light strikes on the surface and further more due to highly expanded and porous structure of graphite and nonwoven as a base, interfaces rapidly transfer of electron in its conductive porous structure increase the load of current density and hold for longer time because of high intake ability of nonwoven structure, as shown in I-V curve image of Figure 8D (d), which represents improved efficiency of solar cell, which confirmed the strong chemistry have been developed while without CQDs solar cell showed I-V curve with less efficient.

Higher impedance values are validated, and the generating mechanism is hampered by the CFE substrate's decreased transparency. The incoming light was absorbed by the dye molecules in the nonwoven fiber network made of expanded graphite and excited electrons that were then injected into the conduction band. Some incident photons decay and are insufficiently excited to transport electrons toward the photo anode conduction band. Due to the recombination of these decaying and lower energy electrons with holes at the electrolyte, V_{OC} has diminished. On the other hand, in the photo anode, which enhances the current density of C-DSSC as indicated in I-V findings, the charges that have been

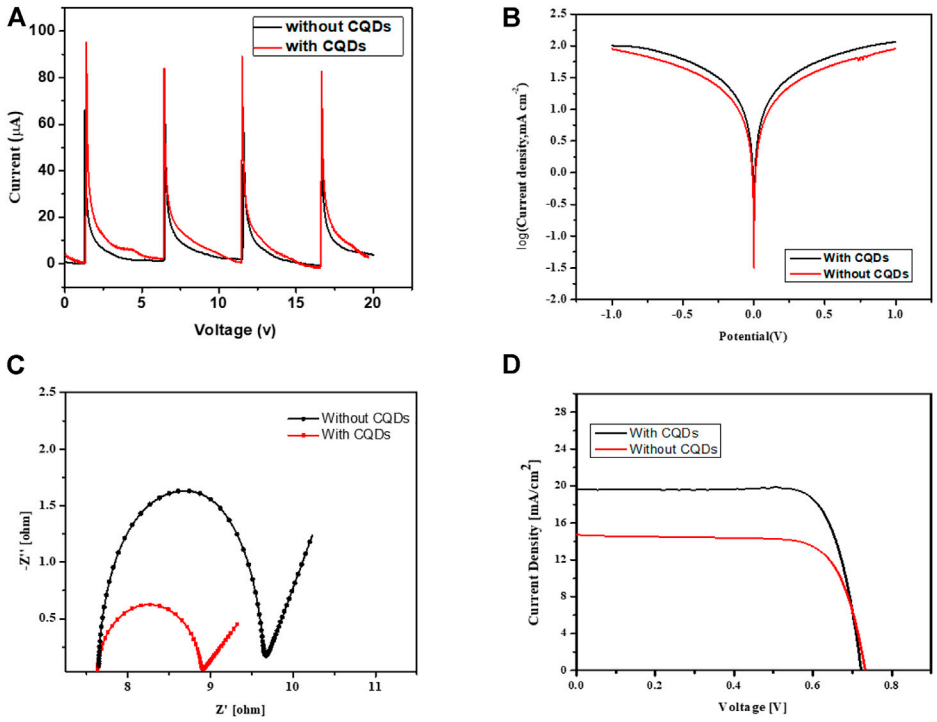

FIGURE 8
(A) Current signal produced while dropping electrolyte on electrode. **(B)** Tafel polarization curves of symmetric cell. **(C)** NY Quist plot for solar cell. **(D)** I-V curve of solar cells with CQDs and without CQDs.

TABLE 1 Comparison of electrochemical and photovoltaic performance of cells fabricated by expanded graphite nonwoven with CQDs and without CQDs electrodes.

Types of DSSC	Symmetrical cells	DSSC				
	R_S [Ω]	R_{CT} [Ω]	Jsc (mA.cm^{-2})	Voc (V)	Fill factor	η% (%)
Expanded graphite with CQDs (TC-DSSC)	7.4	1.25	19.60	0.72	78.94	11.84
Expanded graphite without CQDs (TG-DSSC)	7.6	4.69	14.74	0.73	74.63	8.06

accumulated at the TC-DSSC/CQDs interfaces quickly move towards the load. The I-V curve shows increased cell performance. The I-V curve makes it clear that the photovoltaic performance of solar cells with photo anodes that dip in CQDs with dye is on the rise. The DSSC's total effectiveness increased from 8.06% to 11.84%.

Furthermore, N-CQDs tailored cell photovoltaic performance increased as an increment of TiO_2 coating thickness on an electrode; the coating varied from 6 μm to 10 μm. The increment enabled carrying more CQD particles, increased path voltage, and even overall efficiency of the cell was observed with highly improved efficiency. Here, when N-CQDs tailored light-inducing CEOs are exposed to radiation, both the exchange current density (J0) and the limiting diffusion current density (Jim) increase. J0 = RT/nFRct and Jim = 2nFCDn/l (Guo et al., 2017; Singh and Shougaijam, 2022), where *R* is gas constant, *Ts* absolute temperature, *F* is Faraday's constant, and *l* is the spacer thickness of two electrodes; these light-inducing CEs have enhanced photovoltaic performances in TC-DSSCs (as clearly shown in Table 1). Another comparison was made using a symmetrical solar cell with layers of cathode layer covering both sides (schematic illustration shown in Figure 9) and being at the same level as modern DSSCs (Bai et al., 2014; Guo et al., 2017; Haider et al., 2019; Gao et al., 2021; Singh and Shougaijam, 2022). Overall observation cleared that electron generation and efficiency of the device were enhanced by

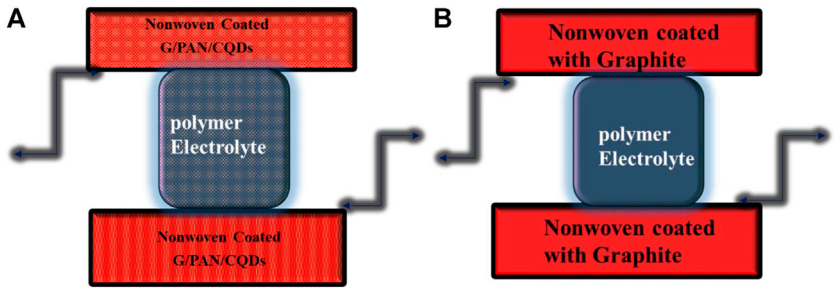

FIGURE 9
Schematic Symmetrical cell comparison **(A)** with CQDs and **(B)** without CQDs.

the right combination of composite with substrate selection. This is one of the approaches to tailor metal-free flexible electrodes. Precursor properties is a key role to improve photovoltaic properties. CQD's characteristic is more identical because of their photo excitation power; however, their stability after 15 days was tested, and their efficiency decreased over time. Further research on this work is required to extend experiments for achieving device more stability and make it applicable on a large scale.

Conclusion

Expanded graphite with CQDs incorporation possesses a high surface area, which enables electrochemical enhanced properties, which is confirmed by morphological and structure analysis. The metal-free device exhibits excellent electrochemical characteristics and more electronic and charge transfer enhancement. Electrochemical results show that, in comparison to TC-DSSC, TG-DSSC exhibits higher electronic and charge transfer efficiency. High charge transfer on a very porous structure demonstrated outstanding electrochemical capabilities, allowing for the proposal of increased solar cell efficiency. Additionally, the comparative study of symmetrical cells was examined by the incorporation of CQDs; the device with CQDs produces high efficiency in comparison to the device without CQDs, and it was discovered that the CQDs' properties are more similar and depend upon their effectiveness in attracting photons. The photoexcitation power of CQDs makes their characteristics more suitable, and, in order for them to be standardized as textile solar cells, the device's flexibility, durability, and washing fastness were tested. The results show that the device is highly flexible and stable in terms of washing fastness. The conductivity is confirmed by highly enlarged porous graphite on nonwoven, which was further improved by the addition of CQDs in photovoltaic testing. The photocatalytic performance revealed 100% photo destruction of methylene blue dye in 25 min.

Data availability statement

The original contributions presented in the study are included in the article/Supplementary Material; further inquiries can be directed to the corresponding author.

Author contributions

All authors listed have made a substantial, direct, and intellectual contribution to the work and approved it for publication.

Funding

This work was supported by the National Natural Science Foundation of China (Nos. 52073166 and 52072226), the Xi'an Key Laboratory of Green Manufacture of Ceramic Materials Foundation (No. 2019220214SYS017CG039), the Key Program for International S&T Cooperation Projects of Shaanxi Province (2020KW-038 and 2020GHJD04), the Science and Technology Program of Xi'an, China (2020KJRC0009), the Scientific Research Program Funded by Shaanxi Provincial Education Department (No. 20JY001), the Science and Technology Resource Sharing Platform of Shaanxi Province (2020 PT-022), and the Science and Technology Plan of Weiyang District, Xi'an (202009).

Acknowledgments

The authors thank the Shaanxi Key Laboratory of Green Preparation and Functionalization for inorganic materials for their experimental platform and testing conditions. Y. Q. Feng was grateful for the support from the Science and

Technology Youth Stars Project of Shaanxi Province (2021KJXX-35).

Conflict of interest

The authors declare that the research was conducted in the absence of any commercial or financial relationships that could be construed as a potential conflict of interest.

Publisher's note

All claims expressed in this article are solely those of the authors and do not necessarily represent those of their affiliated organizations, or those of the publisher, the editors, and the reviewers. Any product that may be evaluated in this article, or claim that may be made by its manufacturer, is not guaranteed or endorsed by the publisher.

References

Ahmed, D. S., Mohammed, M. K. A., and Majeed, S. M. (2020). Green synthesis of eco-friendly graphene quantum dots for highly efficient perovskite solar cells. *ACS Appl. Energy Mat.* 3, 10863–10871. doi:10.1021/acsaem.0c01896

Alley, N. J., Liao, K. S., Andreoli, E., Dias, S., Dillon, E. P., Orbaek, A. W., et al. (2012). Effect of carbon nanotube-fullerene hybrid additive on P3HT:PCBM bulk-heterojunction organic photovoltaics. *Synth. Mater.* 162, 95–101. doi:10.1016/j.synthmet.2011.11.017

Bai, X., Wang, L., Wang, Y., Yao, W., and Zhu, Y. (2014). Enhanced oxidation ability of g-C3N4 photocatalyst via C60 modification. *Appl. Catal. B Environ.* 152–153, 262–270. doi:10.1016/j.apcatb.2014.01.046

Brown, T. M., De Rossi, F., Di Giacomo, F., Mincuzzi, G., Zardetto, V., Reale, A., et al. (2014). Progress in flexible dye solar cell materials, processes and devices. *J. Mat. Chem. A* 2, 10788–10817. doi:10.1039/c4ta00902a

Cao, S., and Yu, J. (2016). Carbon-based H2-production photocatalytic materials. *J. Photochem. Photobiol. C Photochem. Rev.* 27, 72–99. doi:10.1016/j.jphotochemrev.2016.04.002

Fu, X., Xu, L., Li, J., Sun, X., and Peng, H. (2018). Flexible solar cells based on carbon nanomaterials. *Carbon N. Y.* 139, 1063–1073. doi:10.1016/j.carbon.2018.08.017

Gao, K., Gao, X., Zhu, W., Wang, C., Yan, T., Fu, F., et al. (2021). The hierarchical layered microsphere of BiOI x Br 1-x solid solution decorated with N-doped CQDs with enhanced visible light photocatalytic oxidation pollutants. *Chem. Eng. J.* 406, 127155. doi:10.1016/j.cej.2020.127155

Guo, X., Zhang, H., Sun, H., Tade, M. O., and Wang, S. (2017). Green synthesis of carbon quantum dots for sensitized solar cells. *ChemPhotoChem* 1, 116–119. doi:10.1002/cptc.201600038

Haider, Z., Cho, H., Moon, G. hee, and Kim, H. il (2019). Minireview: Selective production of hydrogen peroxide as a clean oxidant over structurally tailored carbon nitride photocatalysts. *Catal. Today* 335, 55–64. doi:10.1016/j.cattod.2018.11.067

He, B., Feng, M., Chen, X., and Sun, J. (2020). Multidimensional (0D-3D) functional nanocarbon: Promising material to strengthen the photocatalytic activity of graphitic carbon nitride. *Green Energy & Environ.* 6, 823–845. doi:10.1016/j.gee.2020.07.011

Heo, J. S., Eom, J., Kim, Y., and Park, S. K. (2018). Recent progress of textile-based wearable electronics: A comprehensive review of materials, devices, and applications. *Small* 14, 1703034. doi:10.1002/smll.201703034

Jiao, Y., Huang, Q., Wang, J., He, Z., and Li, Z. (2019). A novel MoS2 quantum dots (QDs) decorated Z-scheme g-C3N4 nanosheet/N-doped carbon dots heterostructure photocatalyst for photocatalytic hydrogen evolution. *Appl. Catal. B Environ.* 247, 124–132. doi:10.1016/j.apcatb.2019.01.073

Kandi, D., Martha, S., and Parida, K. M. (2017). Quantum dots as enhancer in photocatalytic hydrogen evolution: A review. *Int. J. Hydrogen Energy* 42, 9467–9481. doi:10.1016/j.ijhydene.2017.02.166

Khalid, N. R., Majid, A., Tahir, M. B., Niaz, N. A., and Khalid, S. (2017). Carbonaceous-TiO2 nanomaterials for photocatalytic degradation of pollutants: A review. *Ceram. Int.* 43, 14552–14571. doi:10.1016/j.ceramint.2017.08.143

Khan, M. W., Zuo, X., Yang, Q., Tang, H., Rehman, K. M. U., Wu, M., et al. (2020). Quantum dot embedded N-doped functionalized multiwall carbon nanotubes boost the short-circuit current of Ru (ii) based dye-sensitized solar cells. *Nanoscale* 12, 1046–1060. doi:10.1039/c9nr09227g

Kong, D., Zheng, Y., Kobielusz, M., Wang, Y., Bai, Z., Macyk, W., et al. (2018). Recent advances in visible light-driven water oxidation and reduction in suspension systems. *Mat. TodayKidlingt.* 21, 897–924. doi:10.1016/j.mattod.2018.04.009

Li, K., Su, F., and Zhang, W. (2016). Modification of g-C 3 N 4 nanosheets by carbon quantum dots for highly efficient photocatalytic generation of hydrogen. *Appl. Surf. Sci.* 375, 110–117. doi:10.1016/j.apsusc.2016.03.025

Li, Y., Arumugam, S., Krishnan, C., Charlton, M. D. B., and Beeby, S. P. (2019). Encapsulated textile organic solar cells fabricated by spray coating. *ChemistrySelect* 4, 407–412. doi:10.1002/slct.201803929

Lu, L., Lv, Z., Si, Y., Liu, M., and Zhang, S. (2018). Recent progress on band and surface engineering of graphitic carbon nitride for artificial photosynthesis. *Appl. Surf. Sci.* 462, 693–712. doi:10.1016/j.apsusc.2018.08.131

Lv, B., Feng, X., Lu, L., Xia, L., Yang, Y., Wang, X., et al. (2021). Facile synthesis of g-C3N4/TiO2/CQDs/Au Z-scheme heterojunction composites for solar-driven efficient photocatalytic hydrogen. *Diam. Relat. Mat.* 111, 108212. doi:10.1016/j.diamond.2020.108212

Lv, D., Jiang, Q., Shang, Y., and Liu, D. (2022). Highly efficient fiber-shaped organic solar cells toward wearable flexible electronics. *npj Flex. Electron.* 6, 38–39. doi:10.1038/s41528-022-00172-w

Mahala, C., Sharma, M. D., and Basu, M. (2020). ZnO nanosheets decorated with graphite-like carbon nitride quantum dots as photoanodes in photoelectrochemical water splitting. *ACS Appl. Nano Mat.* 3, 1999–2007. doi:10.1021/acsanm.0c00081

Mousa, S. A., Noby, S. Z., and Shalan, A. E. (2022). "Graphene and its nanocomposites derivatives: Synthesis, properties, and their applications in water treatment, gas sensor, and solar cell fields," in *Advances in nanocomposite materials for environmental and energy harvesting applications* (Springer), 95–128.

Othman, F. E. C., Yusof, N., Jaafar, J., Ismail, A., Hasbullah, H., Abdullah, N., et al. (2016). Preparation and characterization of polyacrylonitrile/manganese dioxides-based carbon nanofibers via electrospinning process. *IOP Conf. Ser. Earth Environ. Sci.* 36, 012006. doi:10.1088/1755-1315/36/1/012006

Peerakiatkhajohn, P., Yun, J.-H., Wang, S., and Wang, L. (2016). Review of recent progress in unassisted photoelectrochemical water splitting: From material modification to configuration design. *J. Photonics Energy* 7, 012006. doi:10.1117/1.jpe.7.012006

Qu, X., Yi, Y., Qiao, F., Liu, M., Wang, X., Yang, R., et al. (2018). TiO2/BiOI/CQDs: Enhanced photocatalytic properties under visible-light irradiation. *Ceram. Int.* 44, 1348–1355. doi:10.1016/j.ceramint.2017.08.185

Ramanujam, J., Bishop, D. M., Todorov, T. K., Gunawan, O., Rath, J., Nekovei, R., et al. (2020). Flexible cigs, CdTe and a-Si: H based thin film solar cells: A review. *Prog. Mat. Sci.* 110, 100619. doi:10.1016/j.pmatsci.2019.100619

Ren, Y., Zeng, D., and Ong, W. J. (2019). Interfacial engineering of graphitic carbon nitride (g-C3N4)-based metal sulfide heterojunction photocatalysts for energy conversion: A review. *Chin. J. Catal.* 40, 289–319. doi:10.1016/s1872-2067(19)63293-6

Riaz, R., Ali, M., Sahito, I. A., Arbab, A. A., Maiyalagan, T., Anjum, A. S., et al. (2019). Self-assembled nitrogen-doped graphene quantum dots (N-GQDs) over graphene sheets for superb electro-photocatalytic activity. *Appl. Surf. Sci.* 480, 1035–1046. doi:10.1016/j.apsusc.2019.02.228

Rotzler, S., Krshiwoblozki, M. von, and Schneider-Ramelow, M. (2021). Washability of e-textiles: Current testing practices and the need for standardization. *Text. Res. J.* 91, 2401–2417. doi:10.1177/0040517521996727

Saberi Motlagh, M., Mottaghitalab, V., Rismanchi, A., Rafieepoor Chirani, M., and Hasanzadeh, M. (2022). Performance modelling of textile solar cell developed by carbon fabric/polypyrrole flexible counter electrode. *Int. J. Sustain. Energy*, 1–21.

Sadasivuni, K. K., Deshmukh, K., Ahipa, T. N., Muzaffar, A., Ahamed, M. B., Pasha, S. K., et al. (2019). Flexible, biodegradable and recyclable solar cells: A review. *J. Mat. Sci. Mat. Electron.* 30, 951–974. doi:10.1007/s10854-018-0397-y

Sahito, I. A., Ahmed, F., Khatri, Z., Sun, K. C., and Jeong, S. H. (2017). Enhanced ionic mobility and increased efficiency of dye-sensitized solar cell by adding lithium

chloride in poly(vinylidene fluoride) nanofiber as electrolyte medium. *J. Mat. Sci.* 52, 13920–13929. doi:10.1007/s10853-017-1473-z

Sahito, I. A., Sun, K. C., Arbab, A. A., Qadir, M. B., Choi, Y. S., and Jeong, S. H. (2016). Flexible and conductive cotton fabric counter electrode coated with graphene nanosheets for high efficiency dye sensitized solar cell. *J. Power Sources* 319, 90–98. doi:10.1016/j.jpowsour.2016.04.025

Sahito, I. A., Sun, K. C., Arbab, A. A., Qadir, M. B., and Jeong, S. H. (2015a). Graphene coated cotton fabric as textile structured counter electrode for DSSC. *Electrochimica Acta* 173, 164–171. doi:10.1016/j.electacta.2015.05.035

Sahito, I. A., Sun, K. C., Arbab, A. A., Qadir, M. B., and Jeong, S. H. (2015b). Integrating high electrical conductivity and photocatalytic activity in cotton fabric by cationizing for enriched coating of negatively charged graphene oxide. *Carbohydr. Polym.* 130, 299–306. doi:10.1016/j.carbpol.2015.05.010

Saravanan, S., Kato, R., Balamurugan, M., Kaushik, S., and Soga, T. (2017). Efficiency improvement in dye sensitized solar cells by the plasmonic effect of green synthesized silver nanoparticles. *J. Sci. Adv. Mater. Devices* 2, 418–424. doi:10.1016/j.jsamd.2017.10.004

Sharif, N. F. M., Shafie, S., Ab Kadir, M. Z. A., Md Din, M. F., Yusuf, Y., and Shaban, S. (2022). TiO2 photoelectrode band gap modification using carbon quantum dots (CQDs) for dye-sensitised solar cells (DSSCs). *Key Engineering Materials* 908, 265–270. doi:10.4028/p-577y33

Singh, S. S., and Shougaijam, B. (2022). Recent development and future prospects of rigid and flexible dye-sensitized solar cell: A review. *Contemp. Trends Semicond. Devices*, 85–109.

Tao, X., Cochrane, C., and Koncar, V. (2019). Launderability of conductive polymer yarns used for connections of e-textile modules: Mechanical stresses. *Fibers Polym.* 20, 2355–2366. doi:10.1007/s12221-019-9325-x

Yang, S., Sun, J., Li, X., Zhou, W., Wang, Z., He, P., et al. (2014). Large-scale fabrication of heavy doped carbon quantum dots with tunable-photoluminescence and sensitive fluorescence detection. *J. Mat. Chem. A* 2, 8660–8667. doi:10.1039/c4ta00860j

Yang, Z., Peng, H., Wang, W., and Liu, T. (2010). Crystallization behavior of poly(ε-caprolactone)/layered double hydroxide nanocomposites. *J. Appl. Polym. Sci.* 116, 2658–2667. doi:10.1002/app.31787

Zhang, Z., Yang, Y., Gao, J., Xiao, S., Zhou, C., Pan, D., et al. (2018). Highly efficient Ag2Se quantum dots blocking layer for solid-state dye-sensitized solar cells: Size effects on device performances. *Mat. Today Energy* 7, 27–36. doi:10.1016/j.mtener.2017.11.005